

PCCP

Accepted Manuscript



This is an *Accepted Manuscript*, which has been through the Royal Society of Chemistry peer review process and has been accepted for publication.

Accepted Manuscripts are published online shortly after acceptance, before technical editing, formatting and proof reading. Using this free service, authors can make their results available to the community, in citable form, before we publish the edited article. We will replace this *Accepted Manuscript* with the edited and formatted *Advance Article* as soon as it is available.

You can find more information about *Accepted Manuscripts* in the [Information for Authors](#).

Please note that technical editing may introduce minor changes to the text and/or graphics, which may alter content. The journal's standard [Terms & Conditions](#) and the [Ethical guidelines](#) still apply. In no event shall the Royal Society of Chemistry be held responsible for any errors or omissions in this *Accepted Manuscript* or any consequences arising from the use of any information it contains.

Coupled-cluster and density functional theory studies of the electronic 0–0 transitions of the DNA bases[†]

Vasily A. Ovchinnikov,^{*ab} and Dage Sundholm^a

Received Xth XXXXXXXXXXXX 20XX, Accepted Xth XXXXXXXXXXXX 20XX

First published on the web Xth XXXXXXXXXXXX 200X

DOI: 10.1039/b000000x

The 0–0 transitions of the electronic excitation spectra of the lowest tautomers of the four nucleotide (DNA) bases have been studied using linear-response approximate coupled-cluster singles and doubles (CC2) calculations. Excitation energies have also been calculated at the linear-response time-dependent density functional theory (TDDFT) level using the B3LYP functional. Large basis sets have been employed for ensuring that the obtained excitation energies are close to the basis-set limit. Zero-point vibrational energy corrections have been calculated at the B3LYP and CC2 levels for the ground and excited states rendering direct comparisons with high-precision spectroscopy measurements feasible. The obtained excitation energies for the 0–0 transitions of the first excited states of guanine tautomers are in good agreement with experimental values confirming the experimental assignment of the energetic order of the tautomers of the DNA bases. For the experimentally detected guanine tautomers, the first excited state corresponds to a $\pi \rightarrow \pi^*$ transition, whereas for the tautomers of adenine, thymine, and the lowest tautomer of cytosine the transition to the first excited state has $n \rightarrow \pi^*$ character. The calculations suggest that the 0–0 transitions of adenine, thymine, and cytosine are not observed in the absorption spectrum due to the weak oscillator strength of the formally symmetry-forbidden transitions, while 0–0 transitions of thymine have been detected in fluorescence excitation spectra.

1 Introduction

Lots of efforts have gone into calculations of vertical excitation energies of the nucleotide (DNA) bases for gaining novel insights into the UV-light initiated photophysical processes of DNA.^{1–21} However, the accuracy of the calculated vertical excitation energies cannot be assessed with high precision by comparing them with ordinary UV-Vis absorption spectra because of the broad band widths of the experimental spectra.^{1,22–24} A huge number of experimental and theoretical studies of electronic excitation processes of the DNA bases have recently been reported^{25–40} and reviewed.^{41–50} When comparing calculated and measured excitation energies, the maximum of the absorption band is usually taken as the vertical excitation energy, which is an assumption that cannot be trusted when aiming at very precise comparisons of calculated and measured values. In high-resolution spectroscopy measurements, the recorded peaks are narrow and correspond to transitions between individual vibrational levels of the ground and excited states.^{51–72} However, the corresponding computational studies are involved, because calcu-

lations of vibrationally resolved electronic transition spectra require optimization of the molecular structure of the ground and excited states. In addition, calculations of the vibrational energies for the initial and final states are also needed. Recent computational studies on small and medium size molecules demonstrated that vibrationally resolved electronic transition energies can be obtained by adding calculated vibrational energies to the energy minima of the two potential energy surfaces.^{73–75} The obtained 0–0 transition energies are useful for assigning high-resolution spectra and for estimating the accuracy of employed computational levels. The peaks of the high-resolution vibrationally resolved spectra are sharp with negligible band widths as compared to the computational accuracy.^{51–72}

Assignments of experimental high-resolution spectra are difficult when there is large number transitions between vibrational levels of several nearly degenerate electronic excited states. For the DNA bases, the first electronic transitions have in general a $n \rightarrow \pi^*$ character implying that they are formally symmetry forbidden with very low peak intensities that render them difficult to detect. There are also other factors that make the detection and assignment of low-lying states difficult. Differences in the molecular structure of the ground and excited states might cause changes in the energetic order of the excited states leading to so-called low-lying conical intersections. When a low-lying conical intersection occurs, the vibrational overtones of the first excited state might become

[†] Electronic Supplementary Information (ESI) available: Cartesian coordinates of the studied molecules. See DOI: 10.1039/b000000x/

^a University of Helsinki, P.O. Box 55 (A.I. Virtanens plats 1), 00014 Helsinki, Finland. Fax: +358 919150279; Tel: +358 449651689; E-mail: vasily@chem.helsinki.fi, Dage.Sundholm@helsinki.fi

^b Emanuel Institute of Biochemical Physics RAS, Kosygin street 4, 119334 Moscow, Russia.

invisible, which causes serious problems to detect the lowest excited state, especially when it corresponds to a dipole-forbidden $n \rightarrow \pi^*$ transition. In such situations, information about the first excited state can be obtained indirectly by measuring the fluorescence excitation spectra, where the quantum yield is enhanced by the deactivation channels of the second excited state through ultrafast internal conversion.^{41,76}

The presence of several tautomers in the sample also introduces problems to assign the high-resolution spectra of the DNA bases, because the vibrationally resolved excitation spectra of the individual tautomers overlap rendering a dense spectrum of sharp peaks. However, spectral hole burning (SHB) experiments and laser induced fluorescence (LIF) measurements enable the assignment of the spectra, because such experiments provide additional information about the energetics and lifetimes of the lowest excited states.^{53,60,61,66}

In this work, the first excited states of a few energetically low-lying tautomers of adenine, thymine, and guanine as well as the two lowest excited states of the four energetically lowest tautomers of cytosine have been studied at the approximate coupled-cluster singles and doubles (CC2) level and at the density functional theory level using Becke's hybrid functional (B3LYP). For higher excited states of the adenine, thymine, and guanine tautomers, conical intersections appear rendering structure optimizations with single reference methods such as CC2 and B3LYP unfeasible.

The paper is organized as follows. In Section 2, we discuss available high-resolution experimental data of relevance for this study. In Section 3, the employed computational methods are presented. In Section 4, the obtained computational results are compared to high-resolution spectroscopy data. The main conclusions are summarized in Section 5.

2 Experimental background

2.1 Adenine

Vibrationally resolved electronic excitation spectra of adenine tautomers have been investigated by several research groups.^{51–58,63,65} Nowak *et al.* showed that only the amino-N(9)H tautomer occurs in argon and nitrogen matrices at low-temperatures.⁵¹ Plützer *et al.* obtained excitation energies for adenine in molecular beams experiments by expanding a mixture of helium and adenine at 210–260 °C.⁵³ By comparing the measured energies with values obtained in calculations, they found that at least two amino-NH tautomers were present in the sample.⁵³ The resonant two-photon ionization (R2PI) spectrum of adenine has a number of resolved vibronic bands in the region between 35500 cm^{-1} and 36770 cm^{-1} , followed by a broad continuous absorption band.⁵⁴ The resolved bands at 35497 cm^{-1} (4.401 eV), 35824 cm^{-1} , 36062 cm^{-1} , 36105 cm^{-1} , and 36248 cm^{-1} denoted A, B, C, D, and E transitions

have been investigated in more detail. According to the assignment of Plützer *et al.*, A, C, D, and E belong to the amino-N(9)H tautomer (**A1**), but originate from different electronic states.^{53,55} The A and C bands originate from the $n \rightarrow \pi^*$ transition. The D band is the origin of $\pi \rightarrow \pi^*$ transition and the E band is due to the $\pi\pi \rightarrow n\pi^*$ vibronic coupling.^{56,57} The B band was shown to belong to the 7H tautomer (**A2**).⁵³ The A band, which is the energetically lowest peak, was suggested to be the 0–0 transition of the amino-N(9)H tautomer.⁵⁴ However, according to Conti *et al.*, the 0–0 transition lying 1000–1200 cm^{-1} (0.124–0.149 eV) lower in energy is not observed experimentally due to its small oscillator strength.⁵⁸ The molecular structures of the studied adenine tautomers are shown in Figure 1.

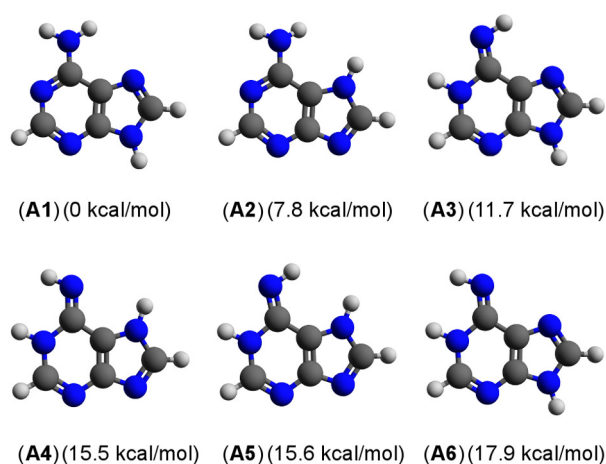


Fig. 1 The six lowest adenine tautomers. The tautomers are ordered according to the ground-state energy calculated at the B3LYP/def2-TZVPPD level. (**A1**) has the lowest total energy of -467.24859 hartree.

2.2 Thymine

The resonance-enhanced multiphoton ionization (REMPI) spectrum of thymine is broad and diffuse despite of jet-cooling.⁵⁹ Tsuchiya *et al.* showed that at least two thymine tautomers are detected in the supersonic jet experiment.⁶⁰ In the fluorescence excitation spectrum of thymine, they found two band systems having well-resolved vibrational structure. The spectrum having the band origin at 33724 cm^{-1} (4.181 eV) was assigned to the 0–0 transition of the diketo tautomer. The band with the origin at 31111 cm^{-1} (3.857 eV) was assigned to the 0–0 transition of one of the keto-enol tautomers, since *ab initio* calculations predicted that the two most stable keto-enol tautomers are 8.5 kcal/mol and 9.4 kcal/mol higher in energy than the diketo tautomer. At experimental condi-

tions with a temperature of 200°C, the concentration of the keto-enol tautomers is expected to be negligibly small.^{60,77} The successful detection of such a small amount of the keto-enol tautomer was ascribed to its very high fluorescence quantum yield. The molecular structures of the studied thymine tautomers are shown in Figure 2.

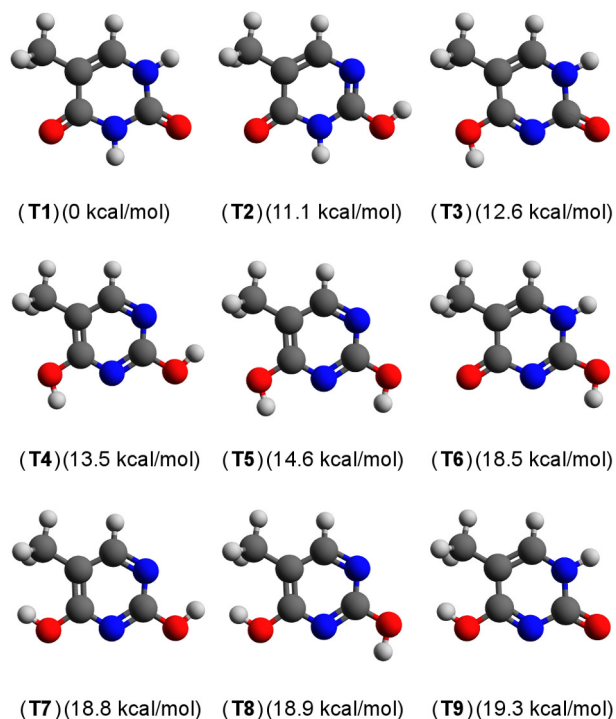


Fig. 2 The nine lowest thymine tautomers. The tautomers are ordered according to the ground-state energy calculated at the B3LYP/def2-TZVPPD level. (T1) has the lowest total energy of -454.08671 hartree.

2.3 Cytosine

Analyzing the REMPI and SHB spectra for cytosine revealed that amino-keto and amino-enol tautomers were present in the supersonic jet experiments.^{61–63} The band origin of the amino-keto tautomer was assigned to the peak at 31826 cm⁻¹ (3.946 eV), which most likely belong to the $\pi \rightarrow \pi^*$ transition. The 0–0 transition of one of the amino-enol tautomers was assigned to the peak at around 36000 cm⁻¹ (4.463 eV).⁶³ Three other tautomers have been identified in supersonic jet and matrix-isolation experiments.⁷⁸ Based on calculated vertical excitation energies, Bazso *et al.* assigned the matrix-isolated UV spectrum as a mixture of the individual spectra of different tautomers.⁷⁸ No transitions from singlet excited states

below 4.5 eV were obtained in the calculations, because they did not consider any changes in the molecular structure of the excited states. Therefore, they draw the incorrect conclusion that a reinterpretation of the REMPI spectrum is necessary. The molecular structures of the studied cytosine tautomers are shown in Figure 3.

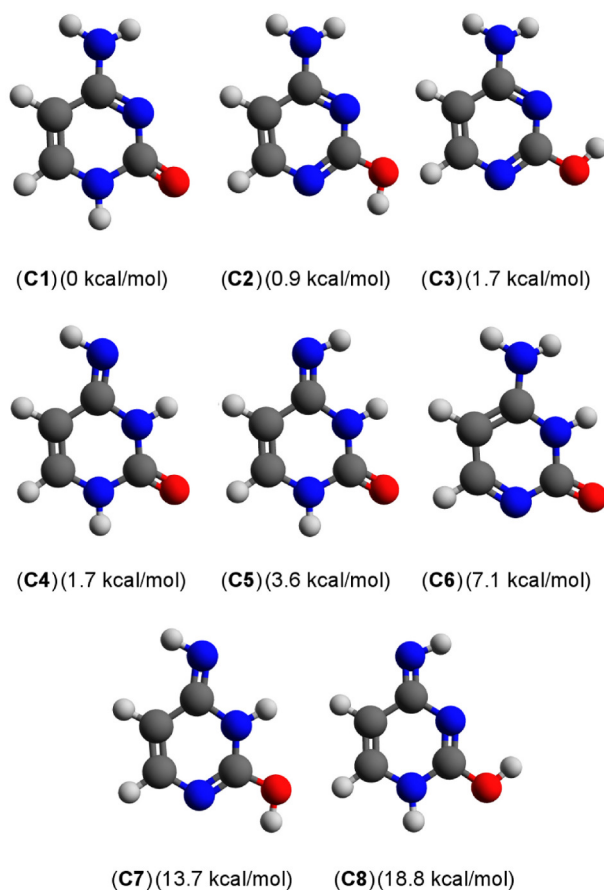


Fig. 3 The eight lowest cytosine tautomers. The tautomers are ordered according to the ground-state energy calculated at the B3LYP/def2-TZVPPD level. (C1) has the lowest total energy of -394.88759 hartree.

2.4 Guanine

The experimental UV and IR spectra of guanine have been investigated more thoroughly than for thymine and cytosine.^{63–72} Nir *et al.* measured the REMPI spectrum of jet-cooled guanine and obtained the lowest peak at 32878 cm⁻¹.⁶⁴ The R2PI, LIF and SHB spectroscopy measurements yielded vibrationally resolved bands of three guanine tautomers with band origins at 32870 cm⁻¹ (4.075 eV),

33274 cm^{-1} (4.125 eV) and 33914 cm^{-1} (4.204 eV), respectively.^{66,67} Mons *et al.* identified bands of the fourth tautomer with the band origin at 34755 cm^{-1} (4.309 eV).⁶⁹ For the other three tautomers, the transition energies measured by Mons *et al.* are systematically 4–6 cm^{-1} smaller than those obtained by Nir *et al.* Using a combination of experimental data and DFT calculations, the experimental assignment of the four tautomers in the supersonic-jet measurement rendered an unambiguous identification of their structures feasible.^{70,72} The four tautomers observed in the R2PI spectrum correspond to (**G5**) with the band origin at 4.075 eV, (**G6**) with the band origin at 4.125 eV, (**G7**) with the band origin at 4.204 eV, and (**G4**) with the band origin at 4.309 eV. The (**G3**) transitions probably occur in the spectrum, since energy barrier for the tautomerization (**G4**) \rightarrow (**G3**) is less than 10 kcal/mol.⁷⁹ The molecular structures of the studied guanine tautomers are shown in Figure 4. In helium nanodroplet experiments, the four observed guanine tautomers correspond to the most stable ones,⁷¹ which is not in agreement with the results obtained in the supersonic-jet measurement.⁷⁰ The reason for the discrepancy between the results obtained in the two experimental studies is that the energetically lowest tautomers have very short-lived excited states and cannot be detected in the R2PI spectrum.^{28,41}

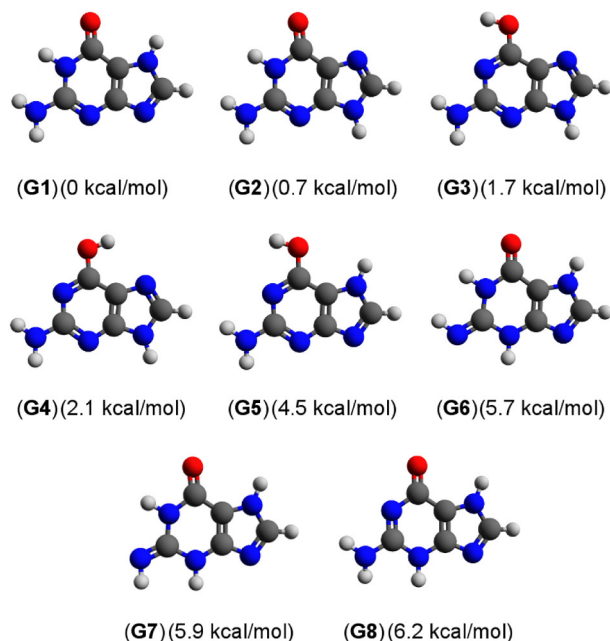


Fig. 4 The eight lowest guanine tautomers. The tautomers are ordered according to the ground-state energy calculated at the B3LYP/def2-TZVPPD level. (**G1**) has the lowest total energy of -542.49074 hartree.

3 Computational details

The molecular structure of the ground states were optimized at the density functional theory (DFT) level using B3LYP functional in combination with the Karlsruhe triple- ζ quality basis sets (def2-TZVP) and the def2-TZVP basis sets augmented with diffuse functions (def2-TZVPPD).^{80–82} The ground-state structures were also optimized at the CC2 level using def2-TZVPPD basis sets.^{83–88} The molecular structures of the excited states were optimized at the time-dependent density functional (TDDFT) level using the B3LYP functional as well as at the linear response CC2 level with the def2-TZVPPD basis sets.^{88–91} No symmetry constraints were imposed. Thus, all calculations were performed in C_1 using the TURBOMOLE program.⁹² All reported structures were confirmed to be minima on the potential energy surface by calculating the vibrational spectra.

To assess the basis set convergence, calculations were also performed using quadruple- ζ quality basis sets (def2-QZVP) and augmented with polarization and diffuse functions (def2-QZVPPD).⁹³ The use of the def2-QZVPPD basis sets did not significantly affect the excitation energies. The results of the basis-set study are summarized in Table 1. Energies for the 0–0 transitions were also calculated at the CC2/def2-TZVPPD level using ground and excited states structures optimized at the B3LYP/def2-TZVPPD level.

The reported CC2 excitation energies are considered reliable when the states have reasonable D_1 and D_2 diagnostic values.^{87,94} From comparisons of calculated and measured excitation energies, we judge that the excitation energy for states with D_1 diagnostic values less than 0.1 and with D_2 diagnostic values less than 0.3 are reliable. As the D_1 and D_2 diagnostic values provide in most cases concordant information about the reliability of the obtained results, a detailed discussion of the D_2 diagnostic values is omitted. The reliability of the calculated CC2 excitation energies have also been judged from comparisons of CC2 and B3LYP excitation energies. When the excitation energies obtained at B3LYP level are larger than the CC2 ones, the CC2 excitation energies are most likely inaccurate as excitation energies are often underestimated at the B3LYP level.

The transition character of the excited states was initially judged from the size of the oscillator strength and then confirmed by visualizing the dominating molecular orbitals of the transitions.

4 Results and discussion

4.1 Adenine

The molecular structure and the relative energies of the six lowest adenine tautomers obtained at the B3LYP/def2-

Table 1 Basis-set study of the vertical excitation energies (in eV) for the two lowest excited singlet states (S_1 and S_2) of tautomers of the DNA bases. The adenine, thymine and cytosine tautomers are the most stable ones, whereas the studied guanine tautomer is the second lowest tautomer. The corresponding oscillator strengths (f) are also reported. The molecular structures were optimized at the B3LYP/def2-TZVP level

Method	State	def2-TZVP	f	def2-TZVPPD	f	def2-QZVP	f	def2-QZVPPD	f
Adenine									
B3LYP	S_1	4.96	0.001	4.93	0.003	4.94	0.002	4.92	0.003
	S_2	5.03	0.187	4.99	0.195	4.99	0.193	4.97	0.198
CC2	S_1	5.19	0.001	5.14	0.002	5.15	0.001	5.13	0.002
	S_2	5.30	0.047	5.27	-0.093	5.26	0.033	5.26	0.291
Thymine									
B3LYP	S_1	4.78	0.000	4.75	0.000	4.76	0.000	4.75	0.000
	S_2	5.03	0.131	4.96	0.129	4.98	0.130	4.95	0.129
CC2	S_1	5.01	0.000	4.95	0.000	4.97	0.000	4.95	0.000
	S_2	5.36	0.186	5.26	0.180	5.29	0.182	5.26	0.179
Cytosine									
B3LYP	S_1	4.71	0.041	4.66	0.043	4.68	0.043	4.66	0.043
	S_2	4.82	0.001	4.80	0.001	4.80	0.001	4.79	0.001
CC2	S_1	4.82	0.056	4.75	0.056	4.77	0.057	4.74	0.057
	S_2	5.06	0.001	5.00	0.002	5.01	0.001	5.00	0.002
Guanine									
B3LYP	S_1	4.92	0.135	4.69	0.031	4.81	0.098	4.64	0.021
	S_2	5.22	0.089	4.87	0.100	5.00	0.041	4.85	0.110
CC2	S_1	5.15	0.170	5.03	0.158	5.06	0.165	5.01	0.159
	S_2	5.60	0.006	5.23	0.006	5.52	0.028	5.23	0.005

TZVPPD level are given in Figure 1. Amino-N(9)H (**A1**) is the energetically lowest tautomer. It is 7.8 kcal/mol below amino-N(7)H (**A2**). The four other tautomers that have imino structures (**A3**)-(**A6**) are more than 10 kcal/mol above (**A1**). The obtained energetic order of the tautomers agrees with previous results.⁵⁵

The transition of the first vertical electronic excitation of (**A1**) and (**A2**) has $n \rightarrow \pi^*$ character, where n is the lone-pair orbital located at the N(1) and N(3) atoms of the purine base. The transition of the first vertical electronic excitation of the (**A3**)-(**A6**) tautomers have $\pi \rightarrow \pi^*$ character. The character of the transition of the two first vertical electronic excitations of (**A1**) and (**A2**) agree with results obtained in previous calculations.^{3-8,12}

Optimization of the molecular structure of the first excited state of the studied tautomers does not affect the character of the transition. For the optimized structure of the first excited state, the transition between the ground state and the first excited state of (**A1**) and (**A2**) has also an $n \rightarrow \pi^*$ character. For (**A3**)-(**A6**), the first excitation is a $\pi \rightarrow \pi^*$ transition. The relative order of the lowest states are schematically described by the potential energy curves in Figure 5b. The vertical excitation energies of the first (S_1) and second (S_2) excited singlet states of the six adenine tautomers are given in Table 2. The reported excitation energies and oscillator strengths were obtained at the CC2/def2-TZVPPD and B3LYP/def2-TZVPPD

levels using the ground-state molecular structures optimized at the B3LYP/def2-TZVP level. The 0-0 transition energies given in Table 3 were obtained by adding the ZPE correction for the ground and excited state to the energy minima of the potential energy surface of the corresponding states.

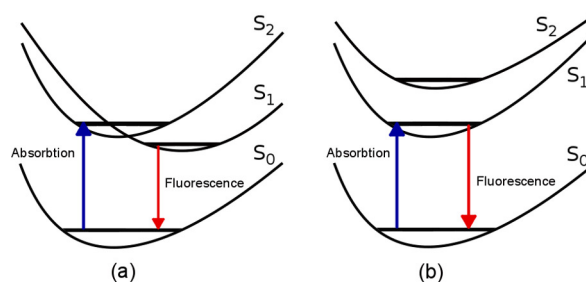


Fig. 5 Excitation and deexcitation pathways of the first excited state of the DNA bases. Scheme (a) shows a low-lying conical intersection where the first and the second excited states appear in different order for the ground and excited state structures. In Scheme (b), there is no crossing of the excited states in the Franck-Condon region.

The D_1 diagnostic values in Table 3 show that the CC2 calculations on the amino tautomers do not suffer from any serious multireference problems, whereas for the imino tau-

Table 2 The vertical excitation energies (in eV) for the two lowest excited singlet states (S_1 and S_2) of the DNA bases tautomers and the corresponding oscillator strengths (f) calculated at the B3LYP/def2-TZVPPD and CC2/def2-TZVPPD levels. The molecular structures were optimized at the B3LYP/def2-TZVP level

Tautomer	S_1				S_2			
	B3LYP	f	CC2	f	B3LYP	f	CC2	f
Adenine								
1	4.93	0.003	5.14	0.002	4.99	0.195	5.27	-0.093
2	4.67	0.005	4.88	0.010	4.92	0.107	5.04	0.116
3	4.26	0.082	4.63	0.095	4.98	0.003	5.35	0.003
4	4.51	0.053	4.89	0.082	4.81	0.003	5.18	0.003
5	4.48	0.057	4.81	0.090	4.78	0.006	5.15	0.007
6	4.26	0.083	4.65	0.096	4.70	0.002	5.10	0.002
Thymine								
1	4.75	0.000	4.95	0.000	4.96	0.129	5.26	0.180
2	4.83	0.163	4.97	0.193	4.92	0.000	5.05	0.000
3	4.50	0.058	4.61	0.071	4.80	0.001	5.00	0.001
4	5.00	0.004	5.08	0.088	5.11	0.087	5.14	0.005
5	4.88	0.004	5.03	0.005	5.08	0.088	5.04	0.090
6	4.43	0.000	4.60	0.000	5.19	0.000	5.35	0.000
7	4.87	0.004	5.01	0.005	5.15	0.078	5.11	0.078
8	4.81	0.004	4.94	0.005	5.13	0.080	5.08	0.081
9	4.51	0.050	4.61	0.063	4.69	0.001	4.88	0.001
Cytosine								
1	4.66	0.043	4.75	0.056	4.80	0.001	5.00	0.002
2	4.97	0.005	5.03	0.101	5.08	0.087	5.11	0.007
3	4.87	0.004	4.99	0.085	5.05	0.090	5.03	0.027
4	4.89	0.129	5.22	0.203	5.22	0.002	5.59	0.004
5	4.93	0.141	5.28	0.210	5.19	0.001	5.61	0.002
6	4.39	0.122	4.30	0.169	4.45	0.002	4.61	0.002
7	4.36	0.080	4.56	0.116	5.13	0.000	5.56	0.000
8	4.58	0.025	4.98	0.031	4.89	0.000	5.39	0.000
Guanine								
1	4.61	0.106	4.84	0.144	4.93	0.007	5.29	0.000
2	4.69	0.031	5.03	0.158	4.87	0.100	5.23	0.006
3	4.70	0.129	4.86	0.117	5.11	0.001	5.40	0.001
4	4.67	0.143	4.83	0.131	5.07	0.001	5.31	0.002
5	4.36	0.076	4.53	0.089	4.84	0.001	5.06	0.002
6	4.23	0.069	4.65	0.110	4.91	0.000	5.20	0.000
7	4.31	0.071	4.79	0.111	4.94	0.000	5.23	0.000
8	4.45	0.000	4.70	0.000	5.04	0.190	5.32	0.257

tomers, the D_1 values are larger than 0.1, which indicates some multireference problems. For (A4) and (A5) the structure optimization of the first excited state failed because of a conical intersection with the ground state. For (A3) and (A6), the CC2 calculations on the imino tautomers using the molecular structure optimized at the B3LYP level yielded acceptable D_1 values of ≤ 0.1 . For (A4) and (A5), the D_1 values of 0.12 are somewhat larger than our accepted upper bound, suggesting that the calculated excitation energies are less reliable than for the other tautomers. However, comparisons of the B3LYP and CC2 excitation energies does not indicate any major problems for the reported CC2 results.

Depending on the employed molecular structure, the 0–0 transition energy of (A1) calculated at the CC2 level is 0.075–0.096 eV below the first peak in the experimental spectrum. Since the transition has $n \rightarrow \pi^*$ character with a very low intensity, the peak at 4.401 eV might originate from a vibronic overtone of the transition as proposed by Conti *et al.*,⁵⁸ even though the deviation between calculated and measured excitation energies is of the same magnitude as the standard deviation for CC2 calculations in the benchmark study.⁷⁵ For the imino tautomers, the 0–0 transition energies calculated at the B3LYP and CC2 levels are less 4 eV. See Table 3. In the supersonic jet experiment, no peaks were detected in this part of the spectrum, which suggests that the imino tautomers were not present in supersonic-jet experiment.

4.2 Thymine

The molecular structures of the nine lowest tautomers of thymine are shown in Figure 2. The tautomer energies relative to the lowest diketo tautomer (T1) are also given in the figure. The second-lowest tautomer is a keto-enol tautomer (T2) lying 11.1 kcal/mol higher in energy as obtained at the B3LYP/def2-TZVPPD level. The (T3) tautomer is energetically only 1.5 kcal/mol above (T2). However, the energy barrier for the tautomerization from (T1) to (T3) is calculated to be 1.2 kcal/mol lower than for the (T1) to (T2) reaction.⁷⁷ Therefore, it is likely that (T3) instead of (T2) is detected in the fluorescence excitation spectrum.⁶⁰ One keto-enol tautomer lying 18.6 kcal/mol above (T1) is not reported because the calculations of the molecular structure of the first excited state was not successful. The B3LYP optimization led to a conical intersection with the ground state and the CC2 calculations suffered from bad D_1 diagnostic values.

The vertical excitation energies and oscillator strengths of the investigated thymine tautomers are given in Table 2. B3LYP calculations show that the transition of the first vertical electronic excitation of (T1), (T4)–(T8) has an $n \rightarrow \pi^*$ character. For (T1) and (T6), n is the lone-pair orbital located at the oxygen atom close to the methyl group, whereas for (T4), (T5), (T7), and (T8), n is the lone-pair orbital at the nitrogen

atoms. For the other tautomers, the transition of the first vertical electronic excitation has $\pi \rightarrow \pi^*$ character. Calculations at the CC2 level yielded the same results except for (T4), the first transition of which has $\pi \rightarrow \pi^*$ character. The transition character of the two lowest vertical electronic excitations of (T1) agrees with the ones obtained in previous calculations.^{3–11}

Optimization of the molecular structure of the first excited state of (T2)–(T4) and (T9) led to a change in the transition character from $\pi \rightarrow \pi^*$ to $n \rightarrow \pi^*$ as illustrated in Figure 5a, where n is located at the oxygen atom of the keto group. Thus, the deactivation of the $\pi \rightarrow \pi^*$ state through internal conversion to the $n \rightarrow \pi^*$ state explains the large quantum yield observed in the fluorescence excitation spectrum of the keto-enol tautomers.⁶⁰

The D_1 diagnostic values of 0.07 for the dienol tautomers suggest that the adiabatic excitation energies calculated at the CC2 level are accurate. However, the dienol tautomers, which are more than 13.5 kcal/mol above (T1) in energy have not been observed experimentally.^{59,60} The other tautomers have conjugated double bonds that lead to molecular structures of the excited state that require multireference wave functions for a proper description. The calculated 0–0 transition energies for thymine are compared to experimental data in Table 4. The present calculations suggest that (T3) is the keto-enol tautomer that is detected in the fluorescence excitation spectrum by Tsuchiya *et al.*⁶⁰

4.3 Cytosine

The molecular structure of the eight studied cytosine tautomers are shown in Figure 3. The difference in the energies between the six lowest tautomers is less than 7 kcal/mol as obtained at the B3LYP/def2-TZVPPD level. The remaining two tautomers that correspond to the imino-enol type are 13.7 kcal/mol and 18.8 kcal/mol higher than (C1) in energy, respectively.

Calculations of the vertical excitation energies at the CC2 level given in Table 2 show that the transition of the first vertical electronic excitation of all studied cytosine tautomers are of $\pi \rightarrow \pi^*$ type, which is also in agreement with previous calculations.^{2–10} At the B3LYP level, the transition to the first excited state of (C2) and (C3) has $n \rightarrow \pi^*$ character, where n is the lone-pair orbital located at the nitrogen atoms of the pyrimidine ring.

For (C1), (C4)–(C6), and (C8), the optimization of the molecular structure of the first excited state at the B3LYP level changes the character of transition between the ground and the first excited state from $\pi \rightarrow \pi^*$ to $n \rightarrow \pi^*$. See Table 5. The potential energy curves for the lowest state of these tautomers are schematically displayed in Figure 5a. The excitation energies for many of the tautomers calculated at the CC2 level are not reliable because of the significant degree of multicon-

Table 3 The first 0–0 transition energies (in eV) for the studied adenine tautomers. The transition character, oscillator strength (f), as well as D_1 and D_2 diagnostic values are also reported.

Tautomer	S_1 type	B3LYP	f	CC2 ^a	D_1	D_2	CC2 ^b	D_1	D_2	Exp. ^c
1	$n \rightarrow \pi^*$	4.166	0.001	4.305	0.07	0.28	4.326	0.07	0.24	4.401
2	$n \rightarrow \pi^*$	3.980	0.002	4.089	0.08	0.26	4.139	0.09	0.29	-
3	$\pi \rightarrow \pi^*$	3.501	0.032	3.537	0.12	0.35	3.620	0.10	0.34	-
4	$\pi \rightarrow \pi^*$	3.703	0.023	-	-	-	3.819	0.12	0.30	-
5	$\pi \rightarrow \pi^*$	3.702	0.019	-	-	-	3.807	0.12	0.32	-
6	$\pi \rightarrow \pi^*$	3.500	0.033	3.525	0.13	0.34	3.613	0.10	0.33	-

^a Excitation energies calculated from optimized at CC2/def2-TZVPPD ground and first excited states structures, with CC2 ZPE corrections.

^b Excitation energies calculated from optimized at B3LYP/def2-TZVPPD ground and first excited states structures, with B3LYP ZPE corrections.

^c Ref.⁵⁴

Table 4 The first 0–0 transition energies (in eV) for the studied thymine tautomers. The transition character, oscillator strength (f), as well as D_1 and D_2 diagnostic values are also reported.

Tautomer	S_1 type	B3LYP	f	CC2 ^a	D_1	D_2	CC2 ^b	D_1	D_2	Exp. ^c
1	$n \rightarrow \pi^*$	4.033	0.000	3.673 ^d	0.19	0.49	3.852 ^d	0.11	0.35	4.181
2	$n \rightarrow \pi^*$	4.149	0.001	3.620 ^d	0.19	0.43	3.817 ^d	0.12	0.38	-
3	$n \rightarrow \pi^*$	3.668	0.000	3.131 ^d	0.15	0.45	3.326 ^d	0.12	0.41	3.857
4	$n \rightarrow \pi^*$	4.281	0.003	4.358	0.07	0.26	4.389	0.07	0.25	-
5	$n \rightarrow \pi^*$	4.168	0.002	4.225	0.08	0.27	4.261	0.07	0.27	-
6	$n \rightarrow \pi^*$	3.760	0.000	3.111 ^d	0.22	0.45	3.437 ^d	0.11	0.37	-
7	$n \rightarrow \pi^*$	4.187	0.002	4.259	0.07	0.25	4.279	0.07	0.24	-
8	$n \rightarrow \pi^*$	4.111	0.002	4.152	0.07	0.26	4.199	0.07	0.26	-
9	$n \rightarrow \pi^*$	3.580	0.000	2.996 ^d	0.16	0.46	3.178 ^d	0.12	0.42	-

^a Excitation energies calculated from optimized at CC2/def2-TZVPPD ground and first excited states structures, with CC2 ZPE corrections.

^b Excitation energies calculated from optimized at B3LYP/def2-TZVPPD ground and first excited states structures, with B3LYP ZPE corrections.

^c Ref.⁶⁰

^d The CC2 excitation energy might be inaccurate because it is smaller than the corresponding B3LYP energy.

figuration character as indicated by the D_1 diagnostic values. Many of the calculated CC2 excitation energies for cytosine are also smaller than the B3LYP excitation energies, which also suggests that there are problems with the CC2 calculations. This also holds when using the molecular structures of the excited states optimized at the B3LYP level in the CC2 calculations. The transition characters of the first excited states obtained at the CC2 and B3LYP levels are though the same.

For (C1) and (C6), the lone-pair orbital is located at the oxygen atom. The optimized molecular structure of the second excited state of (C1) confirms that there is a low-lying conical intersection between its first and second excited state that leads to a change in the character of the ground-state transition. Nir *et al.* detected some weak bands below the origin of the $\pi \rightarrow \pi^*$ transition,⁶¹ which can be assigned to vibronic overtones of the lowest $n \rightarrow \pi^*$ transition. The origin of the transition can probably be detected using fluorescence excitation spectroscopy.

For (C4), (C5), and (C8), the lone-pair orbital is located at the nitrogen atom of imino group, whose hydrogen is oriented perpendicularly to the molecular plane in the optimized first excited state, implying that (C4) and (C5) have identical molecular structures in the first excited state. Deactivation of the vertically excited $\pi \rightarrow \pi^*$ state of the (C4) and (C5) tautomers through internal conversion to the $n \rightarrow \pi^*$ state leads to tautomerization. The molecular structures of the first excited state of (C4) and (C5) is close to a conical intersection that leads to the ground state. However, energetically it is still 1 eV above the ground state. Structure optimization of the first excited state of (C8) at the CC2 level failed because it has a conical intersection with the ground state. However, at the B3LYP level, the optimization of the first excited state of (C8) was successful yielding a structure that is only 0.69 eV above the ground state.

For (C2) and (C3), the optimization of the molecular structure of the first excited state did not change the character of the ground-state transition, which is of $n \rightarrow \pi^*$ and $\pi \rightarrow \pi^*$ type at the B3LYP and CC2 levels, respectively. The oscillator strengths obtained in the CC2 calculations using the optimized CC2 structures of the first excited state are 0.033 for (C2) and 0.017 for (C3), which are significantly smaller than the oscillator strengths that were obtained for the ground-state structures. In the CC2 calculations, the D_1 diagnostic values for (C2) and (C3) are ≤ 0.1 . Since the band origin of the $\pi \rightarrow \pi^*$ transition of one of the amino-enol tautomers has not been experimentally assigned, it is difficult to judge whether the transition to the optimized first excited state is of $n \rightarrow \pi^*$ or $\pi \rightarrow \pi^*$ character. The (C2) tautomer can most likely be detected using REMPI spectroscopy. However, the origin of the first transition is significantly below 35430 cm^{-1} , which the lower end of the energy range of the reported experimental spectrum.⁶¹

For (C3), calculations at the B3LYP level yielded a ground-state transition to the second excited state of $\pi \rightarrow \pi^*$ type, whereas structure optimizations at the CC2 level failed for (C2) and (C3) as well as at the B3LYP level for (C2). The unsuccessful structural optimizations led to a conical intersection between the first and second excited states.

For (C7), the optimization of the molecular structure of the first excited state at the B3LYP level did not change the character of the ground-state transition. In the CC2 calculations, the D_1 diagnostic values are larger than 0.1, also when the molecular structure optimized at the B3LYP level was employed.

4.4 Guanine

The molecular structures of the eight studied guanine tautomers are shown in Figure 4. The energy difference between the first and eighth tautomer is only 6.2 kcal/mol as obtained at the B3LYP level, which agrees with relative energies obtained in previous calculations.²⁷ The other studied guanine tautomers are more than 11 kcal/mol higher than (G1) in energy.²⁷

Calculations of the vertical excitation energies show that the transition character of the first excited state of the seven first guanine tautomers is $\pi \rightarrow \pi^*$. (G8) is the lowest tautomer with the first excited state of $n \rightarrow \pi^*$ type, where the lone-pair orbital is located at the oxygen atom. The obtained character of the ground-state transition for the two lowest vertical excited states of (G2) agrees with the ones reported in previous computational studies.^{3–5} The vertical excitation energies of the studied guanine tautomers are given in Table 2.

The optimization of the molecular structure of the first excited state did not affect the transition character of most of the guanine tautomers. The only exception is (G2). Thus, there is no crossing of the potential energy curves of the lowest excited states as illustrated in Figure 5b. For (G2), the character of the first excited state changes from $\pi \rightarrow \pi^*$ to $\pi \rightarrow R$ when optimizing the molecular structure of the excited state, where R denotes a Rydberg state. The excitation energy of the R state calculated at the B3LYP level is more than 0.6 eV smaller than the CC2 excitation energy indicating computational problems at the B3LYP level. For (G3) and (G4), the structure optimization of the first excited state at CC2 level failed because of a conical intersection with the ground state.

The D_1 diagnostic values of the CC2 calculations are ≤ 0.1 for the optimized molecular structure of the first excited state of (G5)-(G7). The calculated 0–0 transition energies are compared to experimental values in Table 6. When the molecular structure of the first excited state is optimized at the B3LYP/def2-TZVPPD level, the D_1 diagnostic values of the CC2 calculations are ≤ 0.1 for (G2)-(G4). The criteria that CC2 excitation energies must be larger than the B3LYP ones

Table 5 The first 0–0 transition energies (in eV) for the studied cytosine. The transition character, oscillator strength (f), as well as D_1 and D_2 diagnostic values are also reported.

Tautomer	S_1 type	B3LYP	f	CC2 ^a	D_1	D_2	CC2 ^b	D_1	D_2	Exp. ^c
1	$n \rightarrow \pi^*$	3.683	0.000	3.133 ^d	0.15	0.44	3.329 ^d	0.12	0.41	-
2	$n \rightarrow \pi^*$	4.268	0.003	4.318	0.09	0.27	4.342	0.08	0.25	4.463
3	$n \rightarrow \pi^*$	4.169	0.002	4.194	0.08	0.28	4.239	0.08	0.26	-
4	$n \rightarrow \pi^*$	3.060	0.000	2.953 ^d	0.13	0.36	3.031 ^d	0.12	0.35	-
5	$n \rightarrow \pi^*$	2.987	0.000	2.884 ^d	0.13	0.36	2.962 ^d	0.12	0.35	-
6	$n \rightarrow \pi^*$	3.653	0.000	2.974 ^d	0.22	0.46	3.196 ^d	0.14	0.41	-
7	$\pi \rightarrow \pi^*$	3.556	0.013	3.478 ^d	0.14	0.35	3.544 ^d	0.12	0.34	-
8	$n \rightarrow \pi^*$	2.995	0.000	-	-	-	2.913 ^d	0.13	0.36	-
Tautomer	S_2 type	B3LYP	f	CC2 ^a	D_1	D_2	CC2 ^b	D_1	D_2	Exp. ^c
1	$\pi \rightarrow \pi^*$	3.867	0.009	3.639 ^d	0.13	0.42	3.750 ^d	0.11	0.39	3.946
3	$\pi \rightarrow \pi^*$	4.728	0.091	-	-	-	4.756	0.08	0.27	-

^a Excitation energies calculated from optimized at CC2/def2-TZVPPD ground and first excited states structures, with CC2 ZPE corrections.

^b Excitation energies calculated from optimized at B3LYP/def2-TZVPPD ground and first excited states structures, with B3LYP ZPE corrections.

^c Ref. ⁶¹

^d The CC2 excitation energy might be inaccurate because it is smaller than the corresponding B3LYP energy.

and that the D_1 diagnostic value must be smaller than 0.1 yield concordant information about the reliability of the CC2 excitation energies. For (**G1**), the CC2 calculation using the B3LYP optimized structure yielded a 0–0 transition energy that is larger than the one obtained at the B3LYP level, even though the D_1 diagnostic value of 0.11 is slightly outside the acceptable range. Thus, the CC2 excitation energy is probably accurate for the (**G1**) tautomer. According to our CC2 calculations, (**G3**) and (**G4**) have almost the same 0–0 transition energies implying that their spectra might occur in the same energy range of the experimental spectrum. The CC2 excitation energies of the guanine tautomers are in good agreement with the ones deduced from the experimental UV spectrum by Mons *et al.*⁷⁰

5 Summary and conclusions

The ground-state 0–0 transitions of the electronic excitation spectra of the lowest tautomers of adenine, thymine, cytosine, and guanine have been studied at the CC2 level as well as at the TDDFT level using the B3LYP functional. The calculated excitation energies have been compared to experimental values obtained in high-resolution spectroscopy studies. The excitation energies for five states of the DNA bases have a root mean square (RMS) error of 0.099 eV at the CC2 level when the adiabatic excitation energies and the vibrational corrections are calculated for the CC2 optimized molecular structures. An RMS error of 0.063 eV was obtained for six excited states when calculating the adiabatic excitation energies at the CC2 level using the B3LYP optimized structures and vibrational frequencies. Only those of the nine excitation ener-

gies that have reliable CC2 energies were included in the RMS values. The RMS error for the B3LYP excitation energies is 0.292 eV for the nine states. Two of the excitation energies calculated at the B3LYP level deviate more than 0.5 eV from the experimental ones. By omitting the two states, the RMS error of the remaining seven states is 0.161 eV at the B3LYP level. The close agreement between calculated and measured 0–0 transition energies support the experimental assignment of the high-resolution spectra for the DNA bases.

For B3LYP optimized states, the D_1 diagnostic values are in range of 0.07–0.14, which is within the acceptable range of ≤ 0.15 as suggested by Köhn and Hättig,⁸⁷ whereas for excited states optimized at the CC2 level the D_1 diagnostic values are somewhat larger lying in the range of 0.07–0.22. The D_2 diagnostic values are in range of 0.23–0.49, which is outside the recommended range of 0.20–0.25.⁸⁷ However, comparisons with B3LYP and experimental data show that D_2 diagnostic values of 0.30–0.35 can be accepted when the D_1 value does not exceed 0.10.

For adenine, the adiabatic transition to the first excited state of the two lowest tautomers is of $n \rightarrow \pi^*$ type, whereas for the lowest state of the four higher tautomers have excitations of $\pi \rightarrow \pi^*$ character. The first excited state of the two lowest tautomers of adenine was detected experimentally. According to our calculations, the origin band of (**A2**) is energetically lower than for (**A1**).

For thymine, the first adiabatic transition of the nine lowest tautomers are all of $n \rightarrow \pi^*$ character. The first excited state of (**T1**) and (**T3**) have been observed experimentally in fluorescence excitation spectra. Optimization of the molecular structure of the first excited state of (**T3**) change the order of

Table 6 The first 0–0 transition energies (in eV) for the studied guanine. The transition character, oscillator strength (f), as well as D₁ and D₂ diagnostic values are also reported.

Tautomer	S ₁ type	B3LYP	f	CC2 ^a	D ₁	D ₂	CC2 ^b	D ₁	D ₂	Exp. ^c
1	$\pi \rightarrow \pi^*$	4.107	0.103	3.812 ^d	0.21	0.32	4.247	0.11	0.26	-
2	$\pi \rightarrow R$	4.073	0.001	3.747 ^d	0.22	0.34	4.703	0.09	0.23	-
3	$\pi \rightarrow \pi^*$	4.240	0.085	-	-	-	4.261	0.09	0.29	-
4	$\pi \rightarrow \pi^*$	4.251	0.100	-	-	-	4.261	0.09	0.29	4.309
5	$\pi \rightarrow \pi^*$	3.932	0.074	3.997	0.10	0.28	4.046	0.10	0.28	4.075
6	$\pi \rightarrow \pi^*$	3.608	0.016	4.039	0.10	0.31	4.132	0.10	0.33	4.125
7	$\pi \rightarrow \pi^*$	3.640	0.015	4.130	0.10	0.32	4.212	0.10	0.34	4.204
8	$n \rightarrow \pi^*$	3.866	0.000	3.584 ^d	0.19	0.40	3.781 ^d	0.12	0.35	-

^a Excitation energies calculated from optimized at CC2/def2-TZVPPD ground and first excited states structures, with CC2 ZPE corrections.

^b Excitation energies calculated from optimized at B3LYP/def2-TZVPPD ground and first excited states structures, with B3LYP ZPE corrections.

^c Ref. ⁶⁹

^d The CC2 excitation energy might be inaccurate because it is smaller than the corresponding B3LYP energy.

the $\pi \rightarrow \pi^*$ and $n \rightarrow \pi^*$ transitions.

For cytosine, the first adiabatic transition of seven of the eight lowest tautomers are of $n \rightarrow \pi^*$ type. Only for (C7), the first adiabatic transition is of $\pi \rightarrow \pi^*$ type. Comparison with experimental high-resolution spectra of cytosine shows that the first excited state of (C2) and the second excited state of (C1) have been observed spectroscopically. Optimization of the molecular structure of the first excited state of (C1) change the order of the $\pi \rightarrow \pi^*$ and $n \rightarrow \pi^*$ transitions.

For guanine, four tautomers have been assigned in the high-resolution spectra. The calculations suggest that the peaks at around 34500 cm⁻¹ should include the origin of the electronic excitation spectrum of the lowest guanine tautomer. The spectrum is very congested and difficult to assign in that energy range. The spectrum of the second lowest tautomer begins at about 38000 cm⁻¹, which is outside the reported experimental energy range.

The excitation energies calculated at the CC2 level are in good agreement with experimental values with RMS errors of 0.099 eV or 0.063 eV depending on how the vibrational contributions to the excitation energies have been calculated. The excitation energies calculated at the B3LYP level also agree in most cases well with experimental data. However, in a few cases the B3LYP excitation energies are significantly smaller than the experimental and CC2 ones.

The experimental assignment of the energetic order of the tautomers of the DNA bases is confirmed. For the experimentally detected guanine tautomers, the first excited state corresponds to a $\pi \rightarrow \pi^*$ transition, whereas for the studied tautomers of adenine, thymine, and the (C1) tautomer of cytosine, the transition to the first excited state has $n \rightarrow \pi^*$ character.

The calculations suggest that the first 0–0 transitions of adenine and cytosine are not detected experimentally due to the weak oscillator strength of the formally symmetry-forbidden

transitions.

6 Acknowledgement

This research has been supported by Center for International Mobility (CIMO) and the Magnus Ehrnrooth Foundation. It has also been supported by the Academy of Finland through projects (137460 and 266227) and its Computational Science Research Programme (LASTU/258258). CSC – the Finnish IT Center for Science is thanked for computer time.

References

- 1 C. E. Crespo-Hernández, B. Cohen, P. M. Hare and B. Kohler, *Chem. Rev.*, 2004, **104**, 1977–2020.
- 2 R. Bakalska and V. Delchev, *J. Mol. Model.*, 2012, **18**, 5133–5146.
- 3 T. Fleig, S. Knecht and C. Hättig, *J. Phys. Chem. A*, 2007, **111**, 5482–5491.
- 4 L. Jensen and N. Govind, *J. Phys. Chem. A*, 2009, **113**, 9761–9765.
- 5 A. J. A. Aquino, D. Nachtigallová, P. Hobza, D. G. Truhlar, C. Hättig and H. Lischka, *J. Comp. Chem.*, 2011, **32**, 1217–1227.
- 6 M. R. Silva-Junior, M. Schreiber, S. P. A. Sauer and W. Thiel, *J. Chem. Phys.*, 2010, **133**, 174318.
- 7 M. R. Silva-Junior, S. P. Sauer, M. Schreiber and W. Thiel, *Mol. Phys.*, 2010, **108**, 453–465.
- 8 V. Sauri, L. Serrano-Andrés, A. R. M. Shahi, L. Gagliardi, S. Vancoillie and K. Pierloot, *J. Chem. Theory Comput.*, 2011, **7**, 153–168.
- 9 M. Schreiber, M. R. Silva-Junior, S. P. A. Sauer and W. Thiel, *J. Chem. Phys.*, 2008, **128**, 134110.
- 10 P. G. Szalay, T. Watson, A. Perera, V. F. Lotrich and R. J. Bartlett, *J. Phys. Chem. A*, 2012, **116**, 6702–6710.
- 11 M. Etinski, T. Fleig and C. M. Marian, *J. Phys. Chem. A*, 2009, **113**, 11809–11816.
- 12 L. Serrano-Andrés, M. Merchán and A. C. Borin, *Proc. Natl. Acad. Sci. USA*, 2006, **103**, 8691–8696.
- 13 M. K. Shukla and J. Leszczynski, *J. Biomol. Struct. Dyn.*, 2007, **25**, 93–118.
- 14 M. Preuss, W. G. Schmidt, K. Seino, J. Furthmüller and F. Bechstedt, *J. Comp. Chem.*, 2004, **25**, 112–122.

- 15 A. Tsolakidis and E. Kaxiras, *J. Phys. Chem. A*, 2005, **109**, 2373–2380.
- 16 D. Varsano, R. Di Felice, M. A. L. Marques and A. Rubio, *J. Phys. Chem. B*, 2006, **110**, 7129–7138.
- 17 M. Barbatti, A. J. A. Aquino and H. Lischka, *Phys. Chem. Chem. Phys.*, 2010, **12**, 4959–4967.
- 18 A. Tajti, G. Fogarasi and P. G. Szalay, *Chem. Phys. Chem.*, 2009, **10**, 1603–1606.
- 19 M. P. Fülischer, L. Serrano-Andrés and B. O. Roos, *J. Am. Chem. Soc.*, 1997, **119**, 6168–6176.
- 20 M. P. Fülischer and B. O. Roos, *J. Am. Chem. Soc.*, 1995, **117**, 2089–2095.
- 21 J. Lorentzon, M. P. Fülischer and B. O. Roos, *J. Am. Chem. Soc.*, 1995, **117**, 9265–9273.
- 22 D. Voet, W. B. Gratzner, R. A. Cox and P. Doty, *Biopolymers*, 1963, **1**, 193–208.
- 23 L. B. Clark, G. G. Peschel and I. Tinoco, *J. Phys. Chem.*, 1965, **69**, 3615–3618.
- 24 W. Voelter, R. Records, E. Bunnenberg and C. Djerassi, *J. Am. Chem. Soc.*, 1968, **90**, 6163–6170.
- 25 G. Engler, K. Seefeld, M. Schmitt, J. Tatchen, O. Grotkopp, T. J. J. Müller and K. Kleinermanns, *Phys. Chem. Chem. Phys.*, 2013, **15**, 1025–1031.
- 26 I. Pugliesi and K. Müller-Dethlefs, *J. Phys. Chem. A*, 2006, **110**, 13045–13057.
- 27 M. Shukla and J. Leszczynski, *Chem. Phys. Letters*, 2006, **429**, 261–265.
- 28 S. Yamazaki and W. Domcke, *J. Phys. Chem. A*, 2008, **112**, 7090–7097.
- 29 C. M. Marian, *J. Chem. Phys.*, 2005, **122**, 104314.
- 30 S. Perun, A. L. Sobolewski and W. Domcke, *J. Am. Chem. Soc.*, 2005, **127**, 6257–6265.
- 31 L. Blancafort, *J. Am. Chem. Soc.*, 2006, **128**, 210–219.
- 32 S. Perun, A. L. Sobolewski and W. Domcke, *J. Phys. Chem. A*, 2006, **110**, 13238–13244.
- 33 J. J. Serrano-Pérez, R. González-Luque, M. Merchán and L. Serrano-Andrés, *J. Phys. Chem. B*, 2007, **111**, 11880–11883.
- 34 D. Asturiol, B. Lasorne, M. A. Robb and L. Blancafort, *J. Phys. Chem. A*, 2009, **113**, 10211–10218.
- 35 S. Yamazaki and T. Taketsugu, *J. Phys. Chem. A*, 2012, **116**, 491–503.
- 36 M. Merchán, L. Serrano-Andrés, M. A. Robb and L. Blancafort, *J. Am. Chem. Soc.*, 2005, **127**, 1820–1825.
- 37 K. Tomić, J. Tatchen and C. M. Marian, *J. Phys. Chem. A*, 2005, **109**, 8410–8418.
- 38 K. A. Kistler and S. Matsika, *J. Chem. Phys.*, 2008, **128**, 215102.
- 39 L. Blancafort, *Photochem. Photobiol.*, 2007, **83**, 603–610.
- 40 C. G. Triandafillou and S. Matsika, *J. Phys. Chem. A*, 2013, **117**, 12165–12174.
- 41 K. Kleinermanns, D. Nachtigallová and M. S. de Vries, *Intern. Rev. Phys. Chem.*, 2013, **32**, 308–342.
- 42 M. K. Shukla and J. Leszczynski, *WIREs Comput. Mol. Sci.*, 2013, **3**, 637–649.
- 43 L. González, D. Escudero and L. Serrano-Andrés, *Chem. Phys. Chem.*, 2012, **13**, 28–51.
- 44 W. Domcke and D. R. Yarkony, *Annu. Rev. Phys. Chem.*, 2012, **63**, 325–352.
- 45 A. L. Sobolewski and W. Domcke, *Phys. Chem. Chem. Phys.*, 2010, **12**, 4897–4898.
- 46 C. T. Middleton, K. de La Harpe, C. Su, Y. K. Law, C. E. Crespo-Hernández and B. Kohler, *Annu. Rev. Phys. Chem.*, 2009, **60**, 217–239.
- 47 L. Serrano-Andrés and M. Merchán, *J. Photochem. Photobiol. C*, 2009, **10**, 21–32.
- 48 N. Doltsinis, P. L. Markwick, H. Nieber and H. Langer, *Radiation Induced Molecular Phenomena in Nucleic Acids*, Springer Netherlands, 2008, vol. 5, pp. 265–299.
- 49 M. S. de Vries and P. Hobza, *Annu. Rev. Phys. Chem.*, 2007, **58**, 585–612.
- 50 H. Saigusa, *J. Photochem. Photobiol. C*, 2006, **7**, 197–210.
- 51 M. J. Nowak, L. Lapinski, J. S. Kwiatkowski and J. Leszczyński, *J. Phys. Chem.*, 1996, **100**, 3527–3534.
- 52 D. C. Lührs, J. Viallon and I. Fischer, *Phys. Chem. Chem. Phys.*, 2001, **3**, 1827–1831.
- 53 C. Plützer and K. Kleinermanns, *Phys. Chem. Chem. Phys.*, 2002, **4**, 4877–4882.
- 54 N. J. Kim, G. Jeong, Y. S. Kim, J. Sung, S. K. Kim and Y. D. Park, *J. Chem. Phys.*, 2000, **113**, 10051–10055.
- 55 C. Plützer, E. Nir, M. S. de Vries and K. Kleinermanns, *Phys. Chem. Chem. Phys.*, 2001, **3**, 5466–5469.
- 56 N. J. Kim, H. Kang, Y. D. Park and S. K. Kim, *Phys. Chem. Chem. Phys.*, 2004, **6**, 2802–2805.
- 57 Y. Lee, M. Schmitt, K. Kleinermanns and B. Kim, *J. Phys. Chem. A*, 2006, **110**, 11819–11823.
- 58 I. Conti, E. Di Donato, F. Negri and G. Orlandi, *J. Phys. Chem. A*, 2009, **113**, 15265–15275.
- 59 B. B. Brady, L. A. Peteanu and D. H. Levy, *Chem. Phys. Letters*, 1988, **147**, 538–543.
- 60 Y. Tsuchiya, T. Tamura, M. Fujii and M. Ito, *J. Phys. Chem.*, 1988, **92**, 1760–1765.
- 61 E. Nir, M. Müller, L. Grace and M. de Vries, *Chem. Phys. Letters*, 2002, **355**, 59–64.
- 62 E. Nir, I. Hünig, K. Kleinermanns and M. S. de Vries, *Phys. Chem. Chem. Phys.*, 2003, **5**, 4780–4785.
- 63 E. Nir, C. Plützer, K. Kleinermanns and M. S. de Vries, *Eur. Phys. J. D*, 2002, **20**, 317–329.
- 64 E. Nir, L. Grace, B. Brauer and M. S. de Vries, *J. Am. Chem. Soc.*, 1999, **121**, 4896–4897.
- 65 E. Nir, K. Kleinermanns, L. Grace and M. S. de Vries, *J. Phys. Chem. A*, 2001, **105**, 5106–5110.
- 66 F. Piuzzi, M. Mons, I. Dimicoli, B. Tardivel and Q. Zhao, *Chem. Phys.*, 2001, **270**, 205–214.
- 67 E. Nir, C. Janzen, P. Imhof, K. Kleinermanns and M. S. de Vries, *J. Chem. Phys.*, 2001, **115**, 4604–4611.
- 68 W. Chin, M. Mons, I. Dimicoli, F. Piuzzi, B. Tardivel and M. Elhanine, *Eur. Phys. J. D*, 2002, **20**, 347–355.
- 69 M. Mons, I. Dimicoli, F. Piuzzi, B. Tardivel and M. Elhanine, *J. Phys. Chem. A*, 2002, **106**, 5088–5094.
- 70 M. Mons, F. Piuzzi, I. Dimicoli, L. Gorb and J. Leszczyński, *J. Phys. Chem. A*, 2006, **110**, 10921–10924.
- 71 M. Y. Choi and R. E. Miller, *J. Am. Chem. Soc.*, 2006, **128**, 7320–7328.
- 72 K. Seefeld, R. Brause, T. Häber and K. Kleinermanns, *J. Phys. Chem. A*, 2007, **111**, 6217–6221.
- 73 M. Dierksen and S. Grimme, *J. Phys. Chem. A*, 2004, **108**, 10225–10237.
- 74 R. Send, M. Kühn and F. Furche, *J. Chem. Theory Comput.*, 2011, **7**, 2376–2386.
- 75 N. O. C. Winter, N. K. Graf, S. Leutwyler and C. Hättig, *Phys. Chem. Chem. Phys.*, 2013, **15**, 6623–6630.
- 76 C. Canuel, M. Mons, F. Piuzzi, B. Tardivel, I. Dimicoli and M. Elhanine, *J. Chem. Phys.*, 2005, **122**, 074316.
- 77 J.-C. Fan, Z.-C. Shang, J. Liang, X.-H. Liu and H. Jin, *J. Mol. Struct. (Theochem)*, 2010, **939**, 106–111.
- 78 G. Bazsó, G. Tarczay, G. Fogarasi and P. G. Szalay, *Phys. Chem. Chem. Phys.*, 2011, **13**, 6799–6807.
- 79 W. Liang, H. Li, X. Hu and S. Han, *Chem. Phys.*, 2006, **328**, 93–102.
- 80 C. Lee, W. Yang and R. G. Parr, *Phys. Rev. B*, 1988, **37**, 785–789.
- 81 A. D. Becke, *J. Chem. Phys.*, 1993, **98**, 5648–5652.
- 82 D. Rappoport and F. Furche, *J. Chem. Phys.*, 2010, **133**, 134105.
- 83 O. Christiansen, H. Koch and P. Jørgensen, *Chem. Phys. Letters*, 1995, **243**, 409–418.
- 84 F. Weigend and M. Häser, *Theoret. Chem. Acc.*, 1997, **97**, 331–340.
- 85 C. Hättig and F. Weigend, *J. Chem. Phys.*, 2000, **113**, 5154–5161.

-
- 86 F. Weigend, A. Köhn and C. Hättig, *J. Chem. Phys.*, 2002, **116**, 3175–3183.
- 87 A. Köhn and C. Hättig, *J. Chem. Phys.*, 2003, **119**, 5021–5036.
- 88 C. Hättig, *Adv. Quantum Chem.*, 2005, **50**, 37–60.
- 89 R. Bauernschmitt and R. Ahlrichs, *Chem. Phys. Letters*, 1996, **256**, 454–464.
- 90 F. Furche and R. Ahlrichs, *J. Chem. Phys.*, 2002, **117**, 7433–7447.
- 91 F. Furche and R. Ahlrichs, *J. Chem. Phys.*, 2004, **121**, 12772–12773.
- 92 R. Ahlrichs, M. Bär, M. Häser, H. Horn and C. Kölmel, *Chem. Phys. Letters*, 1989, **162**, 165–169.
- 93 F. Weigend, F. Furche and R. Ahlrichs, *J. Chem. Phys.*, 2003, **119**, 12753–12762.
- 94 C. L. Janssen and I. M. B. Nielsen, *Chem. Phys. Letters*, 1998, **290**, 423–430.

Physical Chemistry: Reaction Dynamics

